

The Mass Function of Dark Halos in Superclusters and Voids

E. P. Kurbatov^{1,*}

¹*Institute of Astronomy of the Russian Academy of Sciences*

A modification of the Press–Schechter theory allowing for presence of a background large-scale structure (LSS) – a supercluster or a void is proposed. The LSS is accounted as the statistical constraints in form of linear functionals of the random overdensity field. The deviation of the background density within the LSS is interpreted in a pseudo-cosmological sense. Using the constraints formalism may help us to probe non-trivial spatial statistics of haloes, e.g. edge and shape effects on boundaries of the superclusters and voids. Parameters of the constraints are connected to features of the LSS: its mean overdensity, a spatial scale and a shape, and spatial momenta of higher orders. It is shown that presence of a non-virialized LSS can lead to an observable deviation of the mass function. This effect is exploited to build a procedure to recover parameters of the background perturbation from the observationally estimated mass function.

PACS numbers:

1. INTRODUCTION

Mass function of Press & Schechter [18] (hereafter PS) for dark haloes depends on global cosmological parameters so does not incorporate the presence of the background large-scale disturbances which can form superclusters and voids. Presence of the LSS alter the matter density and can change the growth rate of cosmological fluctuations. This problem was first considered by Bond et al. [2] and Bower [3] as the ‘two barrier’ problem and improved by Mo & White [14], Sheth & Tormen [26], and others. These models provided a connection between the mass function and the background overdensity making possible to solve the inverse problem of recovering the last, as was done by Muñoz & Loeb [15] and Sheth & Diaferio [23]. In these models, however, the background perturbation was considered spherical. Also

* Electronic address: kurbatov@inasan.ru

there was not provided a possibility to examine effects of transition between structures of different densities, e.g. between superclusters and voids.

In this paper a modification of the PS theory is proposed allowing for a background perturbation (name it ‘host’) which is associated with the supercluster or the void. The host perturbation is defined by a set of statistical constraints for the cosmological perturbation field. Growth rate of the random perturbations depends on the host overdensity and determines dynamical age of the population of haloes. As a demonstration of applicability of the model the inverse problem is considered in a simple case for recovering the host overdensity.

Below, in 2nd Section described the modification of the PS theory. In the 3rd Section considered an application of the theory to superclusters and voids. Benefits and issues are discussed in the 4th Section.

2. PRESS–SCHECHTER THEORY WITH STATISTICAL CONSTRAINTS

2.1. *Outline*

The key element of the excursion set theory is the assumption that the virialized haloes form in a hierarchical stochastic process of absorption of haloes of lower masses. Herewith, only those haloes are counted for mass function which are on a top level of a hierarchical tree, i.e. are not sub-haloes of any other halo. The stochastic nature of the process is governed by properties of the initial cosmological fluctuations. Conditions for fluctuations to form a virialized object may be implied to linear stage of their evolution, and with a good approximation they are conditions for the filtered overdensity only. A halo condensed when its characteristic linearly evolved overdensity exceeded some threshold value given from the spherical collapse model. Defining the statistical properties of the fluctuations, their growth rate, and the threshold overdensity allows for completely determining of the function of mass of the haloes for any redshift [2, 11].

The idea is necessary for this research to be done is to describe a large-scale perturbation using formalism of statistical constraints in such a way so that would be possible to define various parameters of the host, e.g. volume averaged density, spatial scale, momenta of inertia etc. The cosmological fluctuations, from which the sub-structures developed, should evolve on top of the background modified by the host. Let’s define ϕ as the residual between a total overdensity field δ and overdensity of the host Δ (which is the ensemble mean for δ ,

and will be defined in Subsec. 2.2.2):

$$\phi(\mathbf{r}) \equiv \delta(\mathbf{r}) - \Delta(\mathbf{r}) , \quad (1)$$

where \mathbf{r} is the spatial position. Also define the field which is filtered over a volume with characteristic scale R :

$$\phi(\mathbf{r}, R) \equiv \int d^3r' W(|\mathbf{r} - \mathbf{r}'|, R) \phi(\mathbf{r}') , \quad (2)$$

where $W(r, R)$ is the filtering function. In a simple approximation all the interesting information on the features of the host contains in variance of the filtered field $\Sigma(\mathbf{r}, R) \equiv \langle \phi^2(\mathbf{r}, R) \rangle$. According to excursion set theory, the hierarchical halo formation process can be interpreted as a random process for the overdensity filtered over the scale R acting as a parameter of the random process. The process starts at the parameter $R = \infty$ moving toward $R = 0$. The mass function can be expressed then via the distribution function for the parameter values when the process first crossed a certain threshold. In presence of the constraints the statistical homogeneity and isotropy of the fluctuations field may be broken and spectral modes of the fluctuations may have non-trivial correlations. Because of this, the excursion set approach in its standard form may not work. This issue will be touched in Subsection 2.2.5.

In theories of PS class the evolution of amplitude of the fluctuations can be accounted either as a time-dependent overdensity threshold or as evolution of the variance. We will stick to the second scheme since it makes possible, in principle, to consider the non-linear corrections to the field evolution. Exact calculation for evolution of the fluctuations' amplitude is difficult even in lowest orders of the perturbation series approach. For Gaussian field these calculations were completed just up to 1-loop corrections, i.e. to 2-nd order of accuracy in power spectrum [10], or up to 3-rd order in expressions for filtered statistical momenta [20]. In a non-gaussian case the task became more complicated since the field has not zero mean so the same precision order requires at least twice as many integrals to get [4, 5]. In our theory we will restrict ourselves to a purely linear evolution, so the overdensity will be proportional to the linear growth factor D :

$$\phi(z, \mathbf{r}) = D(z, \mathbf{r}) \phi_L(\mathbf{r}) . \quad (3)$$

Hereafter the 'L' index means values linearly evolved to the present time with unity growth factor.

The linear evolution of perturbations settled on a large scale host overdensity of both signs (the supercluster or void) can be represented in a perturbation theory for the certain cosmology, which parameters are determined by density of the host. In the overdense host the perturbations will attain higher values of the growth factor than in global cosmology, in the underdense host the last will be lower. Thus, the host overdensity is in charge of the age of haloes population.

It is important to note that all spatial distributions below are defined in a lagrangian coordinates comoving with the matter in modified background. We will distinguish them from the coordinates comoving with the Hubble flow which called the eulerian coordinates.

In this work the Λ CDM model is used with following parameters: $\Omega_{\Lambda,0} = 0.7$, $\Omega_{m,0} = 0.3$, $\sigma_8 = 0.9$. The power spectrum is $P(k) \propto kT^2(k)$, where the transfer function is computed using the Scicmbfast code of Seljak & Zaldarriaga [21]. The units adopted are $h^{-1}M_{\odot}$ for mass, $h^{-1}\text{Mpc}$ for length and $h^{-1}H_{100}^{-1}$ for time, where $H_{100} = 100 \text{ km s}^{-1} \text{ Mpc}^{-1}$.

2.2. Constrained correlation function for modes

To calculate the statistical characteristics such as the variance and the spatial correlation function, we need the correlation function for modes of the constrained field. It's convenient to make calculations using spherical modes decomposition. To obtain the correlation function for amplitudes of the spherical modes we will use approach of Hoffman & Ribak [8], which was proposed by them for plane waves.

The field $\delta(\mathbf{r}) = \delta(r, \boldsymbol{\omega})^1$ can be decomposed to spherical modes via transformation

$$\delta(\mathbf{r}) = \sqrt{\frac{2}{\pi}} \sum_{l=0}^{\infty} \sum_{m=-l}^l \int_0^{\infty} dk k^2 j_l(kr) Y_{lm}(\boldsymbol{\omega}) \tilde{\delta}_{lm}(k), \quad (4)$$

where j_l is the radial Bessel's functions; Y_{lm} is the spherical functions with normalization $\oint_{4\pi} d\omega Y_{lm}^* Y_{l'm'} = 4\pi \delta_{ll'} \delta_{mm'}$. Amplitude of spherical decomposition of the field, or image, is

$$\tilde{\delta}_{lm}(k) = \sqrt{\frac{2}{\pi}} \int_0^{\infty} dr r^2 j_l(kr) \oint_{4\pi} d\omega Y_{lm}^*(\boldsymbol{\omega}) \delta(r, \boldsymbol{\omega}). \quad (5)$$

The image of radially symmetric field $H(r)$ consists of only isotropic modes:

$$\tilde{H}_{lm}(k) = \delta_{l0} \delta_{m0} \tilde{H}(k), \quad (6)$$

¹ The index 'L' is dropped in this Subsection.

where δ_{ij} is the Kronecker's delta, while

$$\tilde{H}(k) = \sqrt{\frac{2}{\pi}} \int_0^\infty dr r^2 j_0(kr) H(r) , \quad (7)$$

$$H(r) = \sqrt{\frac{2}{\pi}} \int_0^\infty dk k^2 j_0(kr) \tilde{H}(k) . \quad (8)$$

Let us write constraints in form of linear functionals, assuming kernels are spherically symmetric and place their centers at origin. Using this conditions, the functional for α -th constraint can be written as

$$C_\alpha[\delta] = \int d^3r H_\alpha(r) \delta(\mathbf{r}) = 4\pi \int_0^\infty dk k^2 \tilde{H}_\alpha(k) \tilde{\delta}_{00}(k) . \quad (9)$$

The constraints itself are fixed by assigning certain values C_α to these functionals. Also the kernels can depend on a set of parameters characterizing the host, like a spatil scale, derivations, or momenta.

Following Hoffman & Ribak [7, 8] it can be showed that the ensemble mean of the constrained field is

$$\Delta(\mathbf{r}) = \langle \delta(\mathbf{r}) | \{C_\alpha\} \rangle , \quad (10)$$

$$\tilde{\Delta}_{lm}(k) = \langle \tilde{\delta}_{lm}(k) | \{C_\alpha\} \rangle = \delta_{l0} \delta_{m0} Q_{\alpha\beta}^{-1} C_\alpha \tilde{\xi}_\beta(k) , \quad (11)$$

where C_α are the values of the constraining functionals; $\tilde{\xi}_\alpha(k)$ are images of cross-correlation function between the field and α -th constraint:

$$\xi_\alpha(\mathbf{r}) = \langle \delta C_\alpha[\delta] \rangle , \quad \tilde{\xi}_\alpha(k) = \tilde{H}_\alpha(k) P(k) ; \quad (12)$$

and $Q_{\alpha\beta}^{-1}$ is the inversion of the constraints' correlation matrix

$$Q_{\alpha\beta} = \langle C_\alpha[\delta] C_\beta[\delta] \rangle = 4\pi \int_0^\infty dk k^2 \tilde{H}_\alpha(k) \tilde{H}_\beta(k) P(k) ; \quad (13)$$

we also can write $Q_{\alpha\beta} = C_\alpha[\xi_\beta]$. It can be showed that the pair correlation function for the constrained ensemble of modes is determined by the residuals:

$$K_{lm'l'm'}(k, k') = \left\langle \tilde{\phi}_{lm}(k) \tilde{\phi}_{l'm'}(k') \right\rangle = \left\langle \left(\tilde{\delta}_{lm}(k) - \tilde{\Delta}_{lm}(k) \right) \left(\tilde{\delta}_{l'm'}(k') - \tilde{\Delta}_{l'm'}(k') \right) \right\rangle , \quad (14)$$

where averaging performed over the non-constrained ensemble. The non-constrained field is delta-correlated, which means

$$\left\langle \tilde{\delta}_{lm}(k) \tilde{\delta}_{l'm'}(k') \right\rangle = \delta_{ll'} \delta_{mm'} \frac{\delta_{1D}(k - k')}{4\pi k k'} P(k) , \quad (15)$$

where δ_{1D} is the one-dimensional Dirac's delta-function. Substituting the definition for ensemble mean field we have

$$K_{lm'l'm'}(k, k') = \delta_{ll'}\delta_{mm'} \frac{\delta_{1D}(k - k')}{4\pi k k'} P(k) - \delta_{l0}\delta_{m0}\delta_{l'0}\delta_{m'0} Q_{\alpha\beta}^{-1} \tilde{\xi}_\alpha(k) \tilde{\xi}_\beta(k'). \quad (16)$$

As can be seen, the presence of constraints leads to fact that the modes are correlated. This changes the spatial statistics of the modes, particularly induces the spatial dependency of the variance. General expression for variance of the filtered field is

$$\Sigma(\mathbf{r}, R) = \langle \phi^2(\mathbf{r}, R) \rangle, \quad (17)$$

where the filtering in spherical decomposition appears in the form

$$\phi(\mathbf{r}, R) = 4\pi \int_0^\infty dk k^2 j_0(kr) \tilde{W}(k, R) \tilde{\phi}_{00}(k). \quad (18)$$

The filter chosen is 'top-hat':

$$W(r, R) = \frac{3}{4\pi R^3} \theta(1 - r/R), \quad (19)$$

$$\tilde{W}(k, R) = \frac{3}{(2\pi)^{3/2}} \frac{\sin kR - kR \cos kR}{(kR)^3}. \quad (20)$$

Substituting (16) into the general expression we obtain

$$\Sigma(\mathbf{r}, R) = S(R) - Q_{\alpha\beta}^{-1} \xi_\alpha(\mathbf{r}, R) \xi_\beta(\mathbf{r}, R), \quad (21)$$

where $S(R)$ denoted the variance of the non-constrained field,

$$S(R) = 4\pi \int_0^\infty dk k^2 \tilde{W}^2(k, R) P(k), \quad (22)$$

and $\xi_\alpha(\mathbf{r}, R)$ is the filtered cross-correlator (12) defined in the same way as in Eq. (18). Because of the constraints the variance becomes dependent on the spatial position. The magnitude of corrections in Eq. (21) decays to zero when $r \rightarrow \infty$. We also may expect this behavior when $R \rightarrow \infty$.

2.3. Constraining kernels and host profile

The amplitude of the mean constrained field or mean overdensity profile is the linear combination of the cross-correlators between the field and the constraints. Choosing appropriate constraining kernel it is possible to set a particular profile for the host. Using set

of the kernels, the mean field can be represented as a combination of some basis profiles. Again, the constraints can be thought of in terms of spatial momenta of the host's density distribution, i.e. average value, moment of inertia, etc.

At the first time consider the single constraint with the top-hat kernel, $H(r, R_H) \equiv W(r, R_H)$. It is easy to see that value of the constraining functional (9) with this kernel fixates the overdensity value averaged over a sphere of radius R_H . Several overdensity constraints applied to different scales $R_{H,\alpha}$ may be combined to obtain more complex profile. In this case the constraining kernels set should be defined as

$$H_\alpha(r) \equiv H(r, R_{H,\alpha}) . \quad (23)$$

The kernels may be choosed to fixate the spatial momenta of different orders:

$$H_\alpha(r) \equiv r^\alpha H(r, R_H) . \quad (24)$$

Yet another possible way to use constraints is to fixate values of the spatial derivations of the host:

$$\begin{aligned} C_\alpha[f] &\equiv C \left[\frac{d^\alpha f}{dr^\alpha} \right] = \int d^3r H(r, R_H) \frac{d^\alpha f(r)}{dr^\alpha} \\ &= (-1)^\alpha \int d^3r \frac{\partial^\alpha H(r, R_H)}{\partial r^\alpha} f(\mathbf{r}) . \end{aligned} \quad (25)$$

The set of the kernels in this case is defined as

$$H_\alpha(r) \equiv (-1)^\alpha \frac{\partial^\alpha H(r, R_H)}{\partial r^\alpha} . \quad (26)$$

Using recurrence relations for radial Bessel functions j_l and their derivations, it can be shown that all the differential constraints of the odd order turn to zero because of symmetry. Images for the second and fourth derivations of the kernel are expressed as

$$\tilde{H}_2(k) = -\frac{k^2}{3} \tilde{H}(k) , \quad \tilde{H}_4(k) = \frac{k^4}{5} \tilde{H}(k) . \quad (27)$$

In this approach the constraints actually fix the moments in the momentum space of the convolved field.

All the examples above were based on the spatially symmertic kernel $H(r, R_H)$. Hence, the ensemble average profile $\Delta(r)$, Eq. (10), has the same property.

From the Eq. (21) it follows that the constraining kernels (but not the values of the constraining functionals) are responsible for corrections to the variance, which is represented

on Fig. 1. On each plot the curves correspond to a fixed radial position inside the host. The farther from the center of the host, the lesser its influence on the filtered field, then the variance turns to its non-constrained form. In the case when filtering spheres are adjusted to the center of the host ($r = 0$), the variance falls to zero for a certain filtering scale. This is the result of using the top-hat constraining kernel, when a value of the filtered overdensity is fixed, i.e. the filtered field loses randomness exactly on the scale $R = R_H$. The several dips appeared when several constraints of a kind (23) are implemented. It was found that applying the derivation constraints (26) does not cause differences from the case of the single overdensity constraint (23), even for higher orders of derivating (not shown on the Fig. 1).

We can go the opposite way, to define the basis profiles then obtain the corresponding set of constraints. Namely, let the cross-correlators $\xi_\alpha(r)$ be the basis profiles. Given values C_β of the constraining functionals, we can express

$$\Delta(r) = Q_{\alpha\beta}^{-1} C_\beta \xi_\alpha(r), \quad (28)$$

where $Q_{\alpha\beta} = C_\alpha[\xi_\beta]$. For example, the profile $\Delta(r)$ could appear from a numerical computations as given, then a single constraint could be generated via this scheme.

Profiles resulting from constraints given above are shown on Fig. 2. In all the cases, except when the momenta constraints used, the volume averaged overdensity (denote it C_0) was set to unity. On top panel the profile resulting from applying four overdensity constraints (23) is presented demonstrating the possibility to model structures having complex form. The computed profiles exhibited moderate variability between nearly zero and unity levels. In contrast, when the momenta constraints were applied, the amplitude of variation was much higher though C_0 was set to 0.1. This suggests that the momenta constraints (24) are hardly suitable for the supercluster profile fitting as the overdensity profile they gave has too strong features to fit.

It is important to note that all the spatial distributions mentioned above are actually defined as a functions of lagrangian coordinates, i.e. comoving with the matter of the growing host. The mass conservation during this process causes displacements of lagrangian elements. Mapping of the lagrangian coordinates to the eulerian ones, i.e. comoving with the Hubble flow, could be followed tracking the evolution of the ‘fluid’ element in a perturbed gravitational field [9]. When the perturbation, the host in our case, has spherical symmetry,

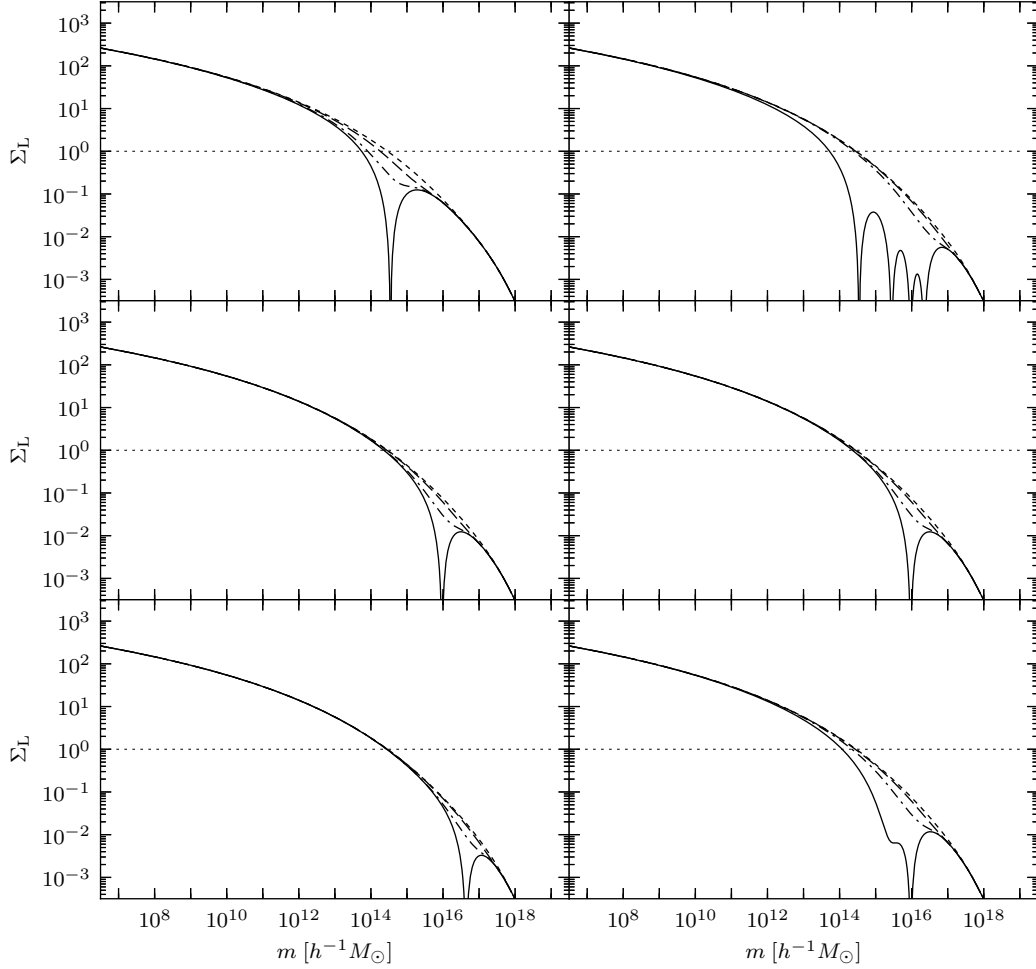


Figure 1. Variance as a function of mass for different sets of constraints. *Left column.* The single top-hat constraint is used. From top to bottom: $R = 10$, $R = 30$, and $R = 50h^{-1}\text{Mpc}$ correspondingly. *Right column.* Top figure: used four top-hat constraints having scales $R = 10, 20, 30, 40h^{-1}\text{Mpc}$. Middle figure: used derivation constraint of the kind (26) for $R = 30h^{-1}\text{Mpc}$. Bottom figure: used momenta constraints of the kind (24) for $R = 30h^{-1}\text{Mpc}$. At all plots solid line is for $r = 0$, long-dash-dotted line is for $r = R/2$, long-dashed line is for $r = R$, and short-dashed represents variance for non-constrained field. In the case of multiple top-hat constraints (right top figure) $R = 40h^{-1}\text{Mpc}$. Thin short-dashed line stands for unity level, the nominal level of non-linearity.

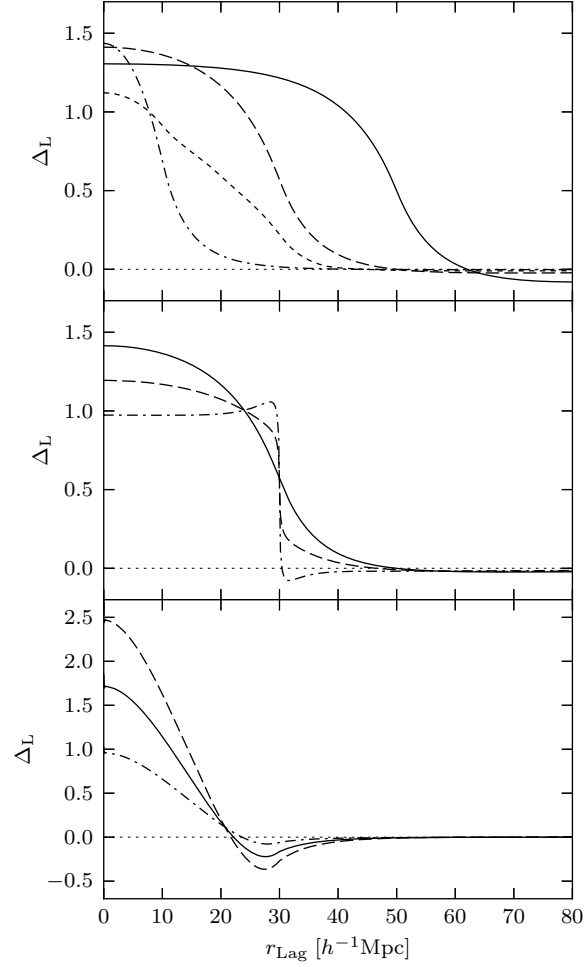


Figure 2. Mean overdensity as a function of lagrangian radial coordinate. These profiles are obtained for different sets of constraints listed in Subsection 2.2.3. *Top panel.* A single top-hat constraint for three values of the scale radius R_H : 50 (solid line), 30 (long-dashed line), and $10h^{-1}\text{Mpc}$ (dot-dashed line). Used the same value of the averaged overdensity 1. With a short-dashed line depicted a distribution with a combination of four top-hat constraints having different scale radii: 10, 20, 30, $40h^{-1}\text{Mpc}$ and corresponding averaged overdensities 1, 0.75, 0.5, and 0.25. *Middle panel.* Derivations constraints of the kind (26) for $\alpha = 0, 2$ and $R_H = 30h^{-1}\text{Mpc}$, where $C_0 = 1$, and C_2 values are 0 (solid line), -0.25 (long-dashed line), -0.5 (dot-dashed line). *Bottom panel.* Momenta constraints of the kind (24) for $\alpha = 0, 1$ and $R_H = 30h^{-1}\text{Mpc}$, where $C_0 = 0.1$, and C_1 values are 0 (solid line), -1 (long-dashed line), 1 (dot-dashed line).

the mapping could be established trivially:

$$r_{\text{eul}}^3(z) = 3 \int_0^{r_{\text{lag}}} dr \frac{r^2}{1 + \Delta(z, r)}. \quad (29)$$

2.4. Linear growth of perturbations

The evolution of perturbations inside an overdense or underdense region can be examined in a pseudo-cosmological notation, if parameters of such notation are chosen appropriately [17, 27]. The parameters are: scale factor, Hubble constant, critical density, and density parameters. For analysis of their dependency on the perturbation overdensity see Martino & Sheth [13]. The brief description is following. The present day value of the scale factor of perturbation a'_0 is determined by the present day amplitude of the region $\bar{\Delta}_0$ as $a'_0 = (1 + \bar{\Delta}_0)^{-1/3}$ while $a' \approx a$, the global scale factor, at early epoch. The Hubble constant H'_0 can be determined implicitly, using these boundary conditions with equation

$$\frac{a}{a'} \frac{da'}{da} = \frac{H'(a'/a'_0, \Omega'_{\text{m},0}, \Omega'_{\Lambda,0})}{H(a, \Omega_{\text{m},0}, \Omega_{\Lambda,0})}, \quad (30)$$

where the present day density parameters of perturbation are

$$\Omega'_{\text{m},0} = (1 + \bar{\Delta}_0) \frac{\Omega_{\text{m},0}}{(H'_0/H_0)^2} \quad \text{and} \quad \Omega'_{\Lambda,0} = \frac{\Omega_{\Lambda,0}}{(H'_0/H_0)^2}. \quad (31)$$

The values found have to be substituted to the linearized equation for overdensity, then the last will be defined relatively to the perturbed background [13]. The linear growth factor D inside the spherical perturbation can be determined via equation

$$a' H' \frac{d}{da'} \left(a' H' \frac{dD}{da'} \right) + 2a' H' \frac{dD}{da'} - \frac{3\Omega'_{\text{m},0} H_0'^2}{2(a'/a'_0)^3} D = 0. \quad (32)$$

The initial condition is the growing mode condition $D \approx a'$ at early epoch, independent on $\bar{\Delta}_0$.

As we are building the local theory, the value of $\bar{\Delta}_0$ should be interpret as a present day non-linear amplitude of the host profile averaged over the volume of the small scale perturbation. However, the statistical constraints applied to the cosmological perturbations result in the host profile at high redshift. Instead of following non-linear evolution of the host, assume the linear approximation (3). The actual host profile at a given redshift will be then

$$\Delta(z, r) = D(z; \bar{\Delta}_0 = 0) \Delta_{\text{L}}(r), \quad (33)$$

where $D(z; \bar{\Delta}_0 = 0)$ is the linear growth factor for the global cosmology, and $\Delta_L(r)$ is the mean overdensity profile (10). Further, to obtain $\bar{\Delta}_0$ the averaging procedure should be applied to this profile at redshift zero.

We assume that the variance of the filtered perturbations (21) seeded inside the host is also governed by the local linear law

$$\Sigma(z, r, R) = D^2(z) \Sigma_L(r, R) , \quad (34)$$

where D is the local growth factor inside the host computed for the corresponding amplitude $\bar{\Delta}_0$ of the host's 'patch' averaged over the sphere R .

2.5. Mass distribution function

In interpretation of Bond et al. [2] for the PS theory, the excursion set formalism relies on two key ideas. First, only those virialized haloes are counted for mass function, which are on a top level of a hierarchical tree, i.e. not sub-haloes of any other halo. Second, the conditions for fluctuations to form a virialized object may be implied to linear stage of their evolution, and with a good approximation they are conditions for the filtered overdensity only. These ideas were successfully realized in terms of a random process for the overdensity $\phi(R)$ filtered over the scale R acting as a parameter of the random process. The process starts at the value 0 and the parameter $R = \infty$ moving toward $R = 0$. The mass function can be expressed then via the distribution function for the parameter values when the process first crossed a certain threshold δ_c . In the absence of constraints the solution for this problem is the PS distribution function (to the correcting factor 'two'):

$$f_S = \frac{\delta_c}{\sqrt{2\pi S^3}} \exp\left(-\frac{\delta_c^2}{2S}\right) , \quad (35)$$

where the variance S used as an equivalent measure of the filtering scale. Bond et al. [2] noted that this random process is not markovian in general, but only if k-sharp filter used. In their paper the authors proposed a procedure to calculate corrections to the PS distribution function for a general filter (see also Maggiore & Riotto [12]). However, in this Paper we will neglect corrections of such kind for simplicity.

In case of a general gaussian random process $\phi(S)$ the distribution function can be written in a form [12]

$$f_S = -\frac{\partial}{\partial S} \int \mathcal{D}[\phi] \exp\left(-\frac{1}{2} \phi^T A^{-1} \phi\right) . \quad (36)$$

This integral is computed over all possible trajectories of the field, not exceeding the threshold δ_c . The look of integration measure $\mathcal{D}[\phi]$ is not important for our study, except it must be positive. The covariance matrix in our case is just

$$A(r, S', S'') = \langle \phi(r, S') \phi(r, S'') \rangle \quad (37)$$

$$= 4\pi \int_0^\infty dk k^2 \tilde{W}(k, S') \tilde{W}(k, S'') P(k) - Q_{\alpha\beta}^{-1} \xi_\alpha(r, S') \xi_\beta(r, S''). \quad (38)$$

Assume firstly the case when $r = 0$ and $\tilde{H}_\alpha(k) = \tilde{W}(k, S_\alpha)$. Denoting $\xi(S', S'') \equiv 4\pi \int_0^\infty dk k^2 \tilde{W}(k, S') \tilde{W}(k, S'') P(k)$ we have $Q_{\alpha\beta} = \xi(S_\alpha, S_\beta)$ and

$$A(0, S', S'') = \xi(S', S'') - Q_{\alpha\beta}^{-1} \xi(S', S_\alpha) \xi(S'', S_\beta). \quad (39)$$

It is obvious that $A(0, S', S_\alpha) \equiv A(0, S_\beta, S'') \equiv 0$, i.e. the covariance matrix has zeroth rows and columns corresponding to each constraining scale. Hence, the inverse of the covariance matrix is singular at the parameters' pairs (S_α, S_β) . For this reason the contribution of the field to the intergral at this points is zero. Due to positiveness of the integrand function, the last is also true for a certain vicinities of these pairs. Thus, the distribution function f_S should turn to zero when $S = S_\alpha$. In a more general case, if $r > 0$, the covariance matrix does not vanish but suppressed at the corresponding rows and columns. This also leads to a suppression of the distribution function at the constraining scales. Indeed, as the mean overdensity has been fixed at a scale S_α , its variance vanishes, so at this scale the structures does not form.

The cross-correlator function $\xi(S', S'')$ behaves roughly like $\min(S', S'')$ (this is exactly true for the k-sharp filter). Hence, at large spatial scales (small variance) the covariance matrix reduces to the non-constrained one (and also the distribution function does). On the other hand, at small spatial scales it tends to the non-constrained matrix, minus some constant amount of order $Q_{\alpha\beta}^{-1} S_\alpha S_\beta$. These limiting cases and all the above suggest us the form of the distribution function preserving the behaviours just investigated. It is the Eq. (35), after substituting the constrained variance Σ instead of the non-constrained S . Taking this as an approximation write out the final definition of the mass PDF which is adopted in subsequent calculations:

$$f_m = \left| \frac{\partial S}{\partial m} \right| \frac{\delta_c}{\sqrt{2\pi\Sigma^3}} \exp\left(-\frac{\delta_c^2}{2\Sigma}\right). \quad (40)$$

Here used the relation between mass and the filtering scale, $m = (4\pi/3) \Omega_{m,0} \rho_{cr,0} R^3$. This mass PDF should be renormalised to unity integral.

Let us summarize the properties of this function. First of all, it depends on spatial position inside the host since the growth factor and the variance depend too. These dependencies are defined by the constraints (or shape of the host profile) as well as their values. Presence of the host itself decreases the variance of the fluctuations' field.

Connection of the background mass distribution to clustering of haloes was considered much earlier by Bond et al. [2] and Bower [3]. Their biased mass PDF can be formally defined as a result of substitutions $\delta_c \mapsto \delta_c - \delta_H$ and $S \mapsto S - S_H$ into the PS distribution (35), where S_H is the non-constrained variance on the scale of the host, and δ_H is the linear overdensity of the host. This result appears in the presented theory as a special case, when the top-hat kernel is used both for single constraint and for filtering, and when the PDF is considered at the centre of the host. In this case the variance reduces to the simple difference $\Sigma = S - S_H$, and the threshold overdensity can be written as the difference noted above when it's expressed relatively to the global density instead of the host's. According to previous authors this special case will be named the extended PS (ePS) model.

Resulting mass PDFs for the single top-hat constraint are shown at Fig. 3. These runs differ by the volume-averaged overdensity and the eulerian radius of the host (according to Eq. (29)). At the first three columns the eulerian radii of the hosts are finite, hence, the effect of modes correlation is on hand appearing as the radial dependence of the shape of the PDF. The most meaningful contrasts between the constrained PDFs and PS one (short-dashed line) is seen for PDFs measured at the centre of the host (solid line), while the outer area of the host has a lesser impact on the modes statistics. Dips and gaps correspond to the mass scale of the entire host. While the gaps are likely artefacts of the spherical top-hat constraint, the certain suppression of the PDF might be a common feature marking the mass scale of the host (e.g. this is the feature of the derivation constraints and momenta constraints also, see Fig. 1 and Subsection 2.2.3). Qualitatively the same result was obtained by Sheth & Tormen [26] where PDF is cut on the host mass scale.

The rightmost column is for a formally 'uniform' limit $R_H \rightarrow \infty$, when the statistics of modes reduces to the non-constrained case, so the population of haloes is affected only through the growth factor. This is also the low mass limit for the PDF.

From the observational point of view the number density of haloes of certain mass is more preferable value than the mass PDF. The number of haloes per unit comoving volume (i.e.

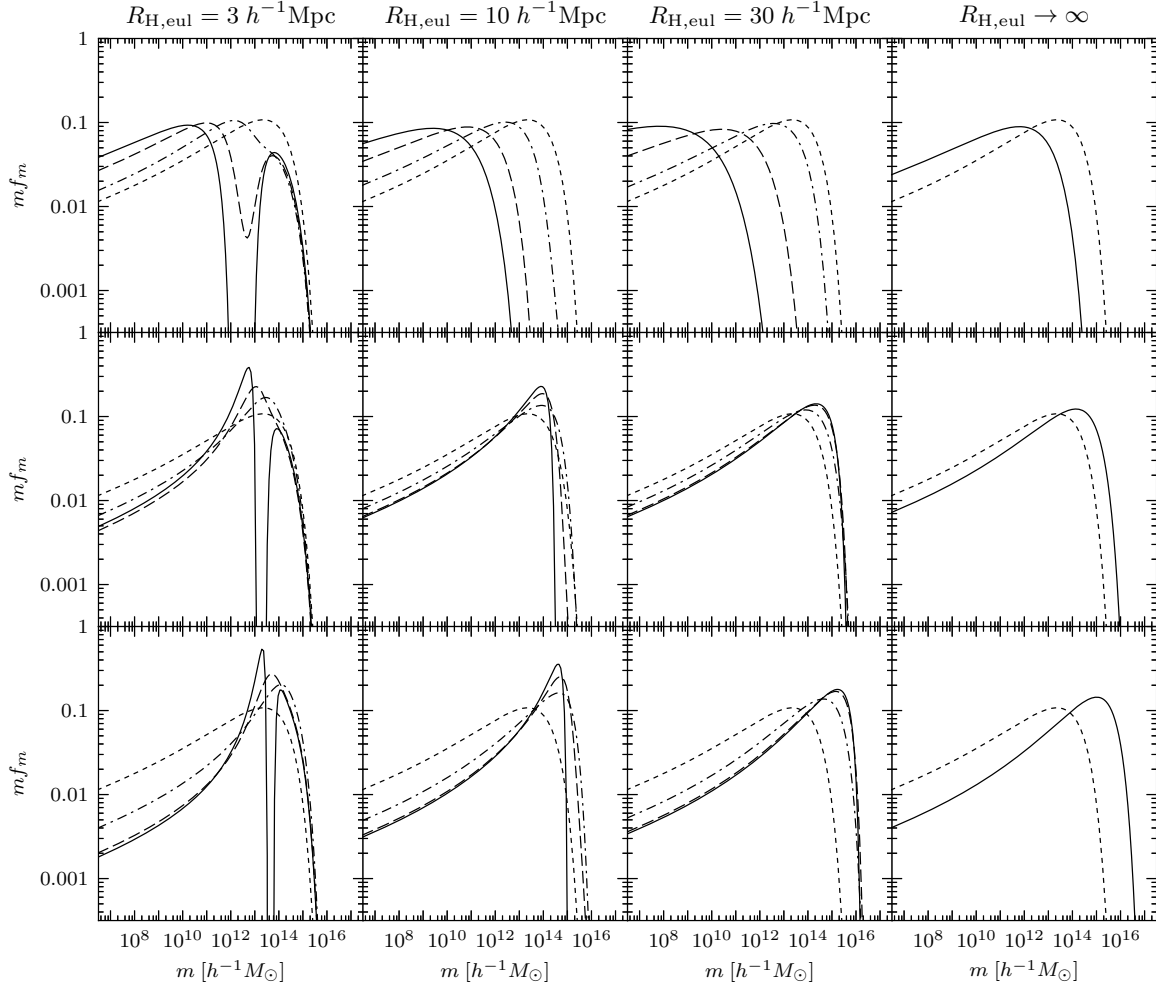


Figure 3. Mass PDF (multiplied by m) at $z = 0$ for a single top-hat constraint having different scales and volume-averaged overdensities. Each row correspond to a certain overdensity $\bar{\Delta}$ (from top to bottom): $-0.65, 1, 4$. Columns from 1 to 3 correspond to a certain constraining scale R_H (from left to right): $3, 10, 30 h^{-1}\text{Mpc}$. On each plot the PDFs is shown for $r = 0$ (solid line), $r = R_H/2$ (long-dashed line), and $r = R_H$ (dot-dashed line). Plots in column 4 correspond to ‘uniform’ case (see text). The short-dashed line stands for non-constrained mass PDF of Press&Schechter.

the lagrangian one) and unit mass is [24]

$$n(z, r, m) = \Omega_{\text{m},0} \rho_{\text{cr},0} \frac{f_m(z, r, m)}{m}. \quad (41)$$

Binding to observational volume, i.e. to the eulerian one, should be done with jacobian of coordinate transformation. In the case of the spherical host the transformation is (29), so

$$n_{\text{eul}} = (1 + \Delta) n.$$

In the cumulative mass function all the strong features of the PDF, like dips, are smoothed when integrating over the volume. The cumulative number of haloes inside a sphere of a given lagrangian radius is

$$N(z, < R_{\text{lag}}, > m) = 4\pi \int_0^{R_{\text{lag}}} dr r^2 \int_m^{m_{\text{lag}}} dm' n(z, r, m'), \quad (42)$$

where $m_{\text{lag}} = (4\pi/3) \Omega_{\text{m},0} \rho_{\text{cr},0} R_{\text{lag}}^3$ is the mass enclosed in the sphere of interest with lagrangian radius R_{lag} . On Fig. 4 depicted the mass CDF for different constraining scales and overdensities. Three classes of models are considered: first where the constraining radius and radius of the sphere of interest are coincide (solid lines), second one when the ‘uniform’ background is used, i.e. constraining radius is infinite (long-dashed lines), and third one correspond to the non-constrained runs. The differences between first two are negligible, except the small sphere of interest case. Deviations from the non-constrained run is significant in all runs. It’s easy to show that on a small scales ($m_{\text{lag}} \ll M_{\text{H}} \equiv (4\pi/3) \Omega_{\text{m},0} \rho_{\text{cr},0} R_{\text{H}}^3$) such a deviation depends on the mean host overdensity only. This behaviour of the mass CDF was well known before as a ‘bias’ [14].

It is important to address the question of scatter in the distribution functions specified above. The scatter can be of two reasons: a deviation of the fluctuations field around the mean profile, and a shot noise in halo counting.

Muñoz & Loeb [15] introduced a method for estimation of the supercluster overdensity in ePS model. Their method based on an assumption that given the host overdensity the number of sub-haloes are distributed accordingly to Poisson law. Connection to the host overdensity was provided with the equation equivalent to (42) but for the mass PDF f_m by Barkana & Loeb [1]. Their model allowed to estimate the sub-haloes number as well as the overdensity scatter inside the host. Let’s evaluate the last for a more general case. Define a distance in a space of profiles using the inversion of the correlation ‘matrix’ (16) as a metric. The square of distance between a trial profile δ and the mean is then

$$\mu^2 = (4\pi)^2 \int_0^\infty dk k^2 \int_0^\infty dk' k'^2 K^{-1}(k, k') \left(\tilde{\delta}(k) - \tilde{\Delta}(k) \right) \left(\tilde{\delta}(k') - \tilde{\Delta}(k') \right), \quad (43)$$

Can be seen that the ‘matrix’ $K(k, k')$ has very strong diagonal so approximately we can write

$$K^{-1}(k, k') \approx \frac{\delta_{1\text{D}}(k - k')}{4\pi k k'} \frac{1}{P(k)}. \quad (44)$$

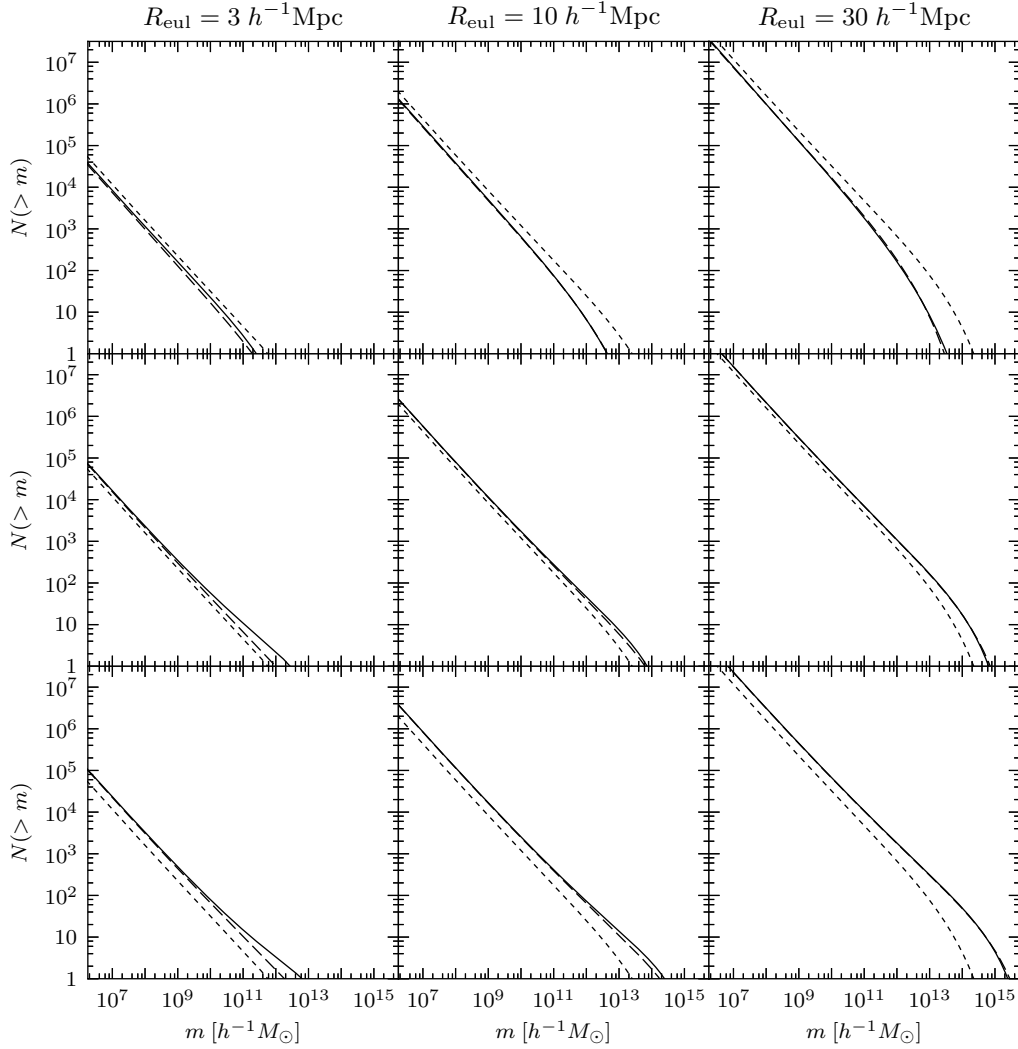


Figure 4. Cumulative mass function. Columns are for three values of the sphere of interest, and rows are for three values of the mean overdensity of the host (the same as Fig. 3). Solid lines show the mass CDF in cases when radius of the sphere of interest coincides with the constraining radius. Long-dashed lines show the models where the constraining radius is infinite, $R_H \rightarrow \infty$. Short-dashed lines show results of the non-constrained runs.

If we determine the trial profile in terms of constraints with kernels h_i , constraints' correlation

matrix q_{ij} , and constraints' values c_i , then the squared distance can be written as

$$\mu^2 = q_{ij}^{-1} c_i c_j + Q_{\alpha\beta}^{-1} C_\alpha C_\beta - 2q_{ij}^{-1} c_i Q_{\alpha\beta}^{-1} C_\alpha 4\pi \int_0^\infty dk k^2 \tilde{h}_j(k) \tilde{H}_\beta(k) P(k). \quad (45)$$

Given the confidence level μ it is possible to restrict the values c_i so the acceptable shapes. As a particular case, if let the profile's deviation to be strictly proportional to the mean profile, the proportionality factor appropriate to the confidence level μ is then $\mu/(Q_{\alpha\beta}^{-1} C_\alpha C_\beta)$. In a purely ePS model (which is equivalent to the case with single top-hat constraint, see above) it's just $\mu\sqrt{S(R_H)}/\bar{\Delta}(R_H)$. Accordingly to Fig. 1, this kind of scatter should not matter much in hosts with enclosed mass $\gtrsim 10^{15} h^{-1} M_\odot$ or equivalent lagrangian scale $\gtrsim 10 h^{-1} \text{Mpc}$.

Another source of scatter arises from the random nature of the excursion process itself. A clustering process was investigated by Sheth [22] then enhanced by Sheth & Pitman [25] and Sheth & Lemson [24]. The approach cited lead to results equivalent to the ePS model Sheth [22]. Let interpret the value of the cumulative mass function $N(> m)$, Eq. (42), as an ensemble mean of a random function $\mathcal{N}(> m)$, which may be represented as a sum over bins of the mass greater than the given, i.e. $\mathcal{N}(> m) = \sum_i \mathcal{N}_i$. Variance of last is then

$$\langle (\mathcal{N}(> m) - N(> m))^2 \rangle = \sum_{i,j} \langle \mathcal{N}_i \mathcal{N}_j \rangle - \sum_{i,j} \langle \mathcal{N}_i \rangle \langle \mathcal{N}_j \rangle. \quad (46)$$

Assuming ePS conditions (there are single top-hat constraint defining a host of a mass M_H) and standing on the Poisson initial distribution approximation [22], the cross-correlator $\langle \mathcal{N}_i \mathcal{N}_j \rangle$ for $i \neq j$ can be expressed in a form similar to eq. (A46) of Sheth & Lemson [24]. For $i = j$ it can be written using their eq. (A49) for $\alpha = 2$. As shown by Sheth & Lemson [24], in a small mass limit, $m \ll M_H$, the cross-correlators decay like $\langle \mathcal{N}_i \mathcal{N}_j \rangle \approx \langle \mathcal{N}_i \rangle \langle \mathcal{N}_j \rangle$ for $i \neq j$, and also $\langle \mathcal{N}_i^2 \rangle \approx \langle \mathcal{N}_i \rangle^2 + \langle \mathcal{N}_i \rangle$. In the opposite limit, $m \sim M_H$, the cross-correlators vanish as well as $\langle \mathcal{N}_i \rangle$. As a result, the poissonian estimation for variance (46) can be quite reliable, i.e.

$$\langle (\mathcal{N}(> m) - N(> m))^2 \rangle \lesssim N(> m). \quad (47)$$

3. RECOVERING PROFILE PARAMETERS OF A HOST

As it turned out, the mass CDF can significantly depend on the host parameters. Consider the possibility to solve the inverse problem, i.e. to recover the host parameters through the

measured cumulative mass function of haloes. The target setting for this inverse problem may be as follows:

- choose a non-virialized structure having spherical shape, or a spherical subvolume;
- choose a set of basis profiles reflecting values we'd like to measure (see Subsec. 2.2.3);
- measure the mass function of virialized substructures inside it, and/or values related to the constraining values;
- adjust theoretical parameters of the host (lagrangian constraining scales and/or constraining values) to fit the theoretical data to the measured data.

Evidently, this inverse problem may be targeted not only to recognize the mean overdensity of the host but also shape and profile details, using a proper set of the host parameters.

To test the method let's focus on a simple case, when we interested in only the volume-averaged overdensity of the host. This problem was already investigated before by Muñoz & Loeb [15] and Sheth & Diaferio [23] as an application to the ePS model to Shapley's supercluster and Sloan Great Wall. Consider the eulerian scale and the mass function at a given redshift are the input parameters. The output will be the host overdensity linearly evolved to the corresponding redshift. Theoretical part herewith is reduced to the case of the single top-hat constraint.

On Fig. 5 is given the number of haloes depending on lower halo mass in the sample, as well as the host overdensity and its scale. Like on the Fig. 4, results of the runs for the finite and infinite-sized hosts are indistinguishable in practice, except for the case $R_{H,eul} = 3 h^{-1}\text{Mpc}$ where the boundary effects play crucial role. As seen, the mapping of the overdensity to the haloes number is not degenerated, though the low density limit is more reliable in sense of the inverse problem.

To successfully apply the method described above, the full lower-bounded by mass sample of haloes is necessary. Another way is to adopt a maximum mass halo to bind the overdensity. As seen on Fig. 6 it is quite sensitive indicator, except for high density case where the represented dependency effectively degenerated.

Both methods for solving the inverse problem are more sensitive with respect to voids rather than superclusters. On the other hand, observational difficulties can somewhat complicate the harvesting of statistics for haloes population. Such difficulties are large spatial

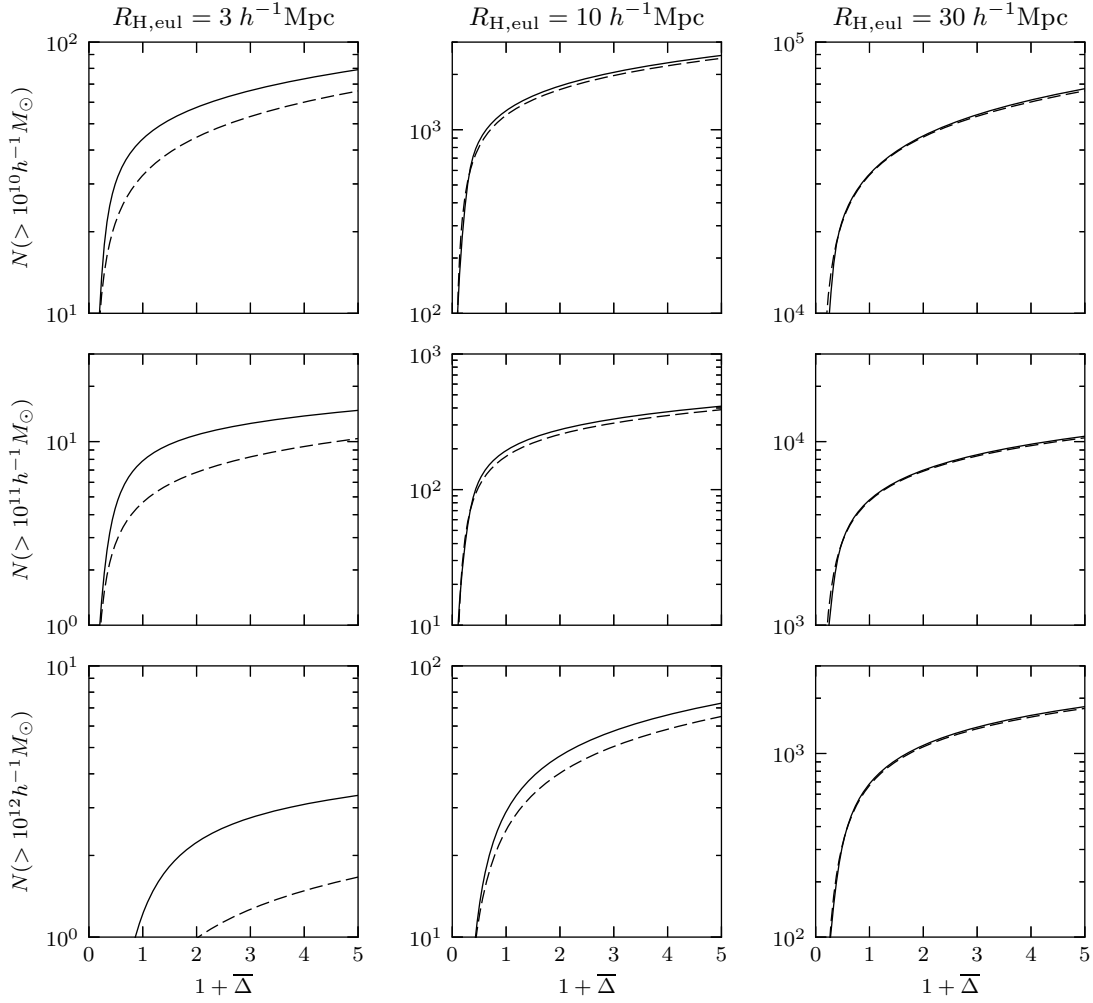


Figure 5. Number of haloes having mass greater than given, as a function of averaged overdensity. The single top-hat constraint is used. Every column correspond to a certain eulerian radius where the mass CDF is computed (the sphere of interest). Solid lines show the case when radius of the sphere of interest coincides with the constraining radius. Long-dashed lines shows the ‘uniform’ models (see text).

extent together with small surface brightness of void galaxies. In spite of this, the methods provided can be helpful for investigation of the problem of voids and superclusters.

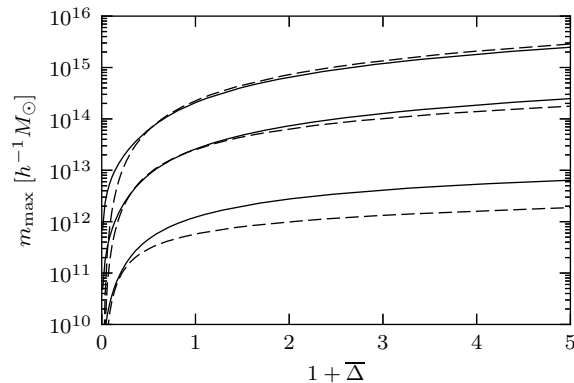


Figure 6. Maximum mass of a halo containing in a host of given eulerian radius, from top to bottom: $30 h^{-1}\text{Mpc}$, $10 h^{-1}\text{Mpc}$, $3 h^{-1}\text{Mpc}$. The styles of lines denote the same as on Fig. 5.

4. DISCUSSION AND CONCLUSION

In this Paper was presented the method for describing the evolution of a virialized halo population in superclusters and cosmological voids. The method is based on the model of Press & Schechter [18] in interpretation of Bond et al. [2] well known as the excursion set formalism. The difference between last and presented model is that the host is described in terms of the statistical constraints implied to the initial overdensity fluctuation field. The constraining procedure used is the method of Hoffman & Ribak [7, 8] reformulated for spherical harmonics. The constraints have form of the linear functionals, and its kernels determine spatial scale and shape of the host perturbation which evolves to the supercluster or void. The model accounted for explicit positional dependency of statistical characteristics of the overdensity field. As a result of imposing the constraints, the characteristics of the statistical field, as well as the halo mass function, clearly become spatially related to the parameters of the background structure. The statistical constraints enable us to specify parameters of the background structure such as the mean density, moments of inertia, gradients, etc.

In the particular cases considered above, the background structure was assumed to be spherically symmetric. However, it is not difficult to generalize our formalism to a structure of arbitrary shape, e.g., a cosmological wall or a filament.

As an application, we have considered the recovery of the mean density of the background structure using both the observed integrated mass function and the mass of the most massive halo. Both formulations yield results that are more sensitive to cosmological voids than

superclusters. On the other hand, the fact that it is difficult to observe galaxies within voids makes the acquisition of reliable halopopulation statistics more complex, since voids are large and sparsely filled, and galaxies within the voids have low surface brightnesses. Nevertheless, this method may be helpful in the study of superclusters and voids.

ACKNOWLEDGMENTS

This work has been funded by grant of the President of Russian Federation for supporting of scientific Schools NSh-3602.2012.2 and also by grant N14.A18.21.1179.

СПИСОК ЛИТЕРАТУРЫ

1. Barkana, R., Loeb, A.: 2004, *Astrophys. J.* 609, 474
2. Bond, J. R., Cole, S., Efstathiou, G., Kaiser, N.: 1991, *Astrophys. J.* 379, 440
3. Bower, R. G.: 1991, *MNRAS* 248, 332
4. Crocce, M., Scoccimarro, R.: 2006, *Phys. Rev. D* 73, 063519
5. Crocce, M., Scoccimarro, R.: 2006, *Phys. Rev. D* 73, 063520
6. Gao, L., White, S. D. M., Jenkins, A., Stoehr, F., Springel, V.: 2004, *MNRAS* 355, 819
7. Hoffman, Y., Ribak, E.: 1991, *Astrophys. J. (Letters)* 380, L5
8. Hoffman, Y., Ribak, E.: 1992, *Astrophys. J.* 384, 448
9. Hui, L., Bertschinger, E.: 1996, *Astrophys. J.* 471, 1
10. Jain, B., Bertschinger, E.: 1994, *Astrophys. J.* 431, 495
11. Lacey, C., Cole, S.: 1993, *MNRAS* 262, 627
12. Maggiore, M., Riotto, A.: 2010, *Astrophys. J.* 711, 907
13. Martino, M. C., Sheth, R. K.: 2009, *MNRAS* 394, 2109
14. Mo, H. J., White, S. D. M.: 1996, *MNRAS* 282, 347
15. Muñoz, J. A., Loeb, A.: 2008, *MNRAS* 391, 1341
16. Navarro, J. F., Frenk, C. S., White, S. D. M.: 1997, *Astrophys. J.* 490, 493
17. Peebles, P. J. E.: 1993, *Principles of physical cosmology*, Princeton University Press, Princeton
18. Press, W. H., Schechter, P.: 1974, *Astrophys. J.* 187, 425
19. Reed, D., Governato, F., Quinn, T., et al.: 2005, *MNRAS* 359, 1537
20. Scoccimarro, R.: 1998, *MNRAS* 299, 1097
21. Seljak, U., Zaldarriaga, M.: 1996, *Astrophys. J.* 469, 437
22. Sheth, R. K.: 1996, *MNRAS* 281, 1277
23. Sheth, R. K., Diaferio, A.: 2011, *MNRAS* 417, 2938
24. Sheth, R. K., Lemson, G.: 1999, *MNRAS* 304, 767
25. Sheth, R. K., Pitman, J.: 1997, *MNRAS* 289, 66
26. Sheth, R. K., Tormen, G.: 1999, *MNRAS* 308, 119
27. Silk, J.: 1977, *Astron. and Astrophys.* 59, 53